Anat Embryol (2001) 204:217–224

ORIGINAL ARTICLE

Martin Leu · Elisabeth Ehler · Jean-Claude Perriard

Characterisation of postnatal growth of the murine heart

Accepted: 26 June 2001

Abstract Using a new technique to isolate rod-shaped cardiomyocytes from small tissue pieces we were able to analyse the developmental profile of postnatal cardiomyocyte growth in the mouse. During the first 4 postnatal days the volume of the cardiomyocytes remains relatively constant despite a concomitant increase in heart weight, indicating growth due to cell division of the cardiomyocytes, also called hyperplasia. After postnatal day 5 the volume of the cardiomyocytes increases dramatically until postnatal day 14, when the increment of the volume curve decreases again. The cardiomyocytes reach their adult volume at around 3 months of age. These measurements present the first detailed analysis of the phase of so-called developmental hypertrophy, i.e. normal cardiomyocyte growth in the mouse, and provide an essential base-line for the analysis of growth parameters in mouse models for cardiomyopathies. We used this method to characterise the growth characteristics of cardiomyocytes from MLP (muscle LIM protein) knockout mice, a mouse model for dilated cardiomyopathy. During the first 2 postnatal weeks there is no significant difference in the growth parameters between MLP knockout and wildtype mice. However, in the adult animals cardiomyocytes from MLP knockout mice are not only characterised by a more irregular shape, but also by a high variability in size compared to cardiomyocytes from wildtype animals. This suggests that the alterations in ventricular morphology in the MLP heart are not due to a general elongation of the cardiomyocytes but to myocyte disarray and ventricular wall thinning caused by the heterogeneous volume of the cardiomyocyte population.

Keywords Cardiomyocytes · Isolation method · Developmental parameters · MLP · Cardiac growth · Hypertrophy

M. Leu · E. Ehler · J.-C. Perriard (✉)
Institute of Cell Biology, ETH Zurich Honggerberg,
CH-8093 Zurich, Switzerland
Tel.: +41-1-6333359, Fax: +41-1-6331069
e-mail: jcp@cell.biol.ethz.ch

Abbreviations *DTT* dithiothreitol · *PFA* paraformaldehyde · *MLP* muscle LIM protein · *PBS* phosphate buffered saline · *BSA* bovine serum albumin · *PIPES* piperazine-N,N'-bis(2-ethanesulfonic acid) · *EGTA* ethylene glycol-bis(b-aminoethyl ether) N,N,N',N' tetraacetic acid · *MES* 2–8(N-morpholino)ethanesulfonic acid monohydrate

Introduction

The heart is the first differentiated organ in the developing embryo. While already performing its function, namely to pump blood, it continues to grow in order to meet increased demands on its working output. In the rat for example, heart weight increases from 33 mg in the newborn to 134 mg in the adult animal (Li et al. 1996). This growth can be achieved by two different means: hyperplasia, i.e. growth due to cell division of cardiomyocytes or hypertrophy, i.e. growth due to volume increase of the individual cardiomyocyte. Pioneering studies by Clubb and Bishop (Clubb and Bishop 1984) have defined three different phases of growth in the rat heart: (1) The hyperplastic phase, which lasts until postnatal day 4 (P4), (2) a transitional phase between P5 and P15 when hyperplasia and hypertrophy would occur concomitantly, and (3) the hypertrophic phase from P15 onwards when growth would be caused solely by addition of myofibrils. Recently Li and colleagues (Li et al. 1996) provided data pointing at a rather sharp transition between hyperplastic and hypertrophic phase in the rat and claimed that the DNA synthesis that was still observed in the first 2 postnatal weeks was mainly due to nuclear division, a common feature of rodent cardiomyocytes, which are mainly binucleated. During puberty the growth of the cardiomyocytes is slowed down until it reaches a plateau in the adult animals. In case of specific physiological requirements because of exercise or due to pathological situations like elevated blood pressure a second phase of hypertrophic growth can set in. The cardiomyocytes then increase their volume further in an

adaptive response by adding more myofibrils and sarcomeres. This process can run out of control and result in a phenotype that is defined as pathological hypertrophy, which will finally lead to heart insufficiency and death.

So far, detailed analysis of cardiac growth parameters has been performed in rat (Li et al. 1996), pig (Beinlich et al. 1995), sheep (Smolich et al. 1989), guinea pig (Campbell et al. 1987), dog (Legato 1979) and chicken (Li et al. 1997), and several species-specific features have been noted, with, for example, chicken cardiomyocytes retaining the ability to divide even in the adult stage similar to amphibian cardiomyocytes (Oberpriller and Oberpriller 1974; Rumyantsev 1977). However, only few data are available for the mouse so far. In view of the fact that more and more mouse models for cardiomyopathies are being studied, it is important to determine the base-line of normal cardiac growth in order to be able to compare potential aberrant growth characteristics of cardiomyocytes from diseased mice with normal mice. One potential explanation for the lack of data for the mouse so far is the size of the tissue compared to larger mammals. Therefore, conventional isolation methods for cardiomyocytes to measure their volume, like retrograde perfusion with collagenase using a Langendorff apparatus cannot be used at early postnatal stages of development. In order to determine the growth parameters during postnatal mouse heart development, we developed a new method that enables us to isolate rod-shaped cardiomyocytes also at very young stages (from P0 onwards) while at the same time allowing us to distinguish between cardiomyocytes from the left and the right ventricle. The volume of these cardiomyocytes was measured by computer analysis of data sets obtained by confocal microscopy.

Using this method we could determine that the phase of hypertrophy sets in at around P5 in the mouse, reaching a plateau in early adulthood. We then employed this technique to analyse the growth parameters of cardiomyocytes from a mouse model for dilated cardiomyopathy, the MLP knockout mouse (Arber et al. 1997). This study revealed that while there are no significant differences between wildtype and MLP knockout cardiomyocytes at early stages of development, cardiomyocytes from adult MLP knockout mice are characterised by a higher variability not only in overall shape but also in size. This provides one potential explanation for the myocyte disarray that is observed in these diseased hearts.

Materials and methods

Cardiomyocyte isolation

Mice were killed by cervical dislocation and the hearts were immediately excised. Cardiomyocytes were enzymatically isolated from mouse (strain C57Bl6; BRL, Füllinsdorf, Switzerland) hearts of different ages (P0 (postnatal day 0) to P205) using an adapted procedure originally developed for smooth muscle cells (Draeger et al. 1989). The left and right ventricular wall was dissected from isolated hearts, and depending on the size, cut into smaller pieces on ice in Solution 1 consisting of (in mmol/l) 137 NaCl, 5 KCl, 4 $NaHCO_3$, 5.5 glucose, 1,1 $Na_2HPO_4x2H_2O$, 0.4 KH_2PO_4, 2 EGTA, 5 MES, 2 $MgCl_2$ and 100 mg/l streptomycin; pH 6.1. The tissue pieces (approximately 1×3 mm) were tied with cotton thread onto plastic strips at extended length (see schematic drawing in Fig. 1) and digested in a buffer solution (pH 6.5) consisting of (in mmol/l) 137 NaCl, 5 KCl, 4 $NaHCO_3$, 5.5 glucose, 10 PIPES, 2.5 $CaCl_2$, 2 $MgCl_2$ and 100 mg/l streptomycin, containing 1 mg/ml collagenase type II (Worthington Biochemical, N.Y. USA) and 1 µg/ml verapamil (Knoll AG, Liestal, Switzerland) at 37°C for 20 min and up to 1.5 h, depending on the age of the mice. After washing three times on ice with washing solution (i.e. Solution 1 without $MgCl_2$ but containing in addition 0.5 mmol/l DTT), the pieces were cut off from the strips and placed in 100 µl–500 µl cold washing solution, depending on the size of the muscle pieces. Final dissociation of cells was performed by gently triturating the heart pieces several times through a wide-mouth Pasteur pipette. The cells were spun on gelatine-coated slides with a cytospin centrifuge (10 s, 500 rpm; Shandon Southern, Pa., USA) and subsequently fixed with 3% PFA in PBS for 15 min at room temperature.

For the analysis of cardiomyocytes from a mouse model with dilated cardiomyopathy, the MLP knockout strain (Arber et al. 1997) and its wildtype strain (OBF E52) were used.

Hearts intended for cryostat sectioning were snap-frozen in isopentane in liquid nitrogen. Then, 10-µm-thick sections were generated using a cryostat, collected on gelatine-coated slides and processed for immunofluorescence as described below.

Immunofluorescence

For the staining with anti-myomesin [monoclonal mouse anti myomesin clone B4 (Grove et al. 1984), characterised in this laboratory] and with Pico Green to visualise the nuclei (Molecular Probes from Juro Supply AG, Luzern, Switzerland), the cells were incubated after fixation with 0.1 mol/l glycine in PBS for 5 min and afterwards permeabilised with 0.2% Triton X-100 in PBS for 15 min. Unspecific binding sites were blocked by incubation with 5% normal (pre-immune) goat serum (Sigma, Buchs, Switzerland), 1% BSA in PBS for 15 min. Primary and secondary antibodies were diluted in blocking solution. The primary antibody incubation was carried out overnight at 4°C and the incubation with the secondary antibody (Cy3 anti mouse Ig; Jackson Immuno Research from Milan, La Roche, Switzerland) and Pico Green, respectively was performed for 2.5 h at room temperature. After three times washing with 0.002% Triton X-100 in PBS for 5 min, the specimens were mounted in 0.1 mol/l TRIS-HCl (pH 9.5) : glycerol (3:7) including 50 mg/ml n-propyl-gallate as anti-fading reagent (Messerli et al. 1993a).

Volume measurements and statistical analysis

The imaging system consisted of a Leica inverted microscope DM IRB/E, a Leica true confocal scanner TCS NT and a Silicon Graphics workstation. The data sets from single isolated cells were recorded from top to bottom of the cell using a Leica PL APO 63x/1.4 oil objective and a Z-axis step size of 0.3 µm. The system was equipped with an argon/krypton mixed gas laser. Image processing was done on a Silicon Graphics workstation using Imaris (Bitplane AG, Zurich, Switzerland), a 3D multi-channel image processing software specialised for confocal microscopy images (Messerli et al. 1993b). The volume was determined on a Silicon Graphics workstation, using the Depth Analysis program that is part of the Imaris software package. The mean volume with the standard deviation (SD) for each data point was obtained using the statistic functions of the KaleidaGraph program (Synergy Software, Pa., USA). At least five cells from two independent isolations were measured for each point.

Results

A novel technique for the isolation of rod-shaped cardiomyocytes from postnatal mouse heart

Conventional isolation of perinatal rodent cardiomyocytes is routinely carried out using two different approaches. One is bulk digestion of tissue in stirred collagenase solution, which usually yields spherical cells that no longer display the shape of cardiomyocytes as seen in the tissue (Rothen-Rutishauser et al. 1998). Freshly isolated cells that maintain their original shape can be obtained by retrograde perfusion with collagenase solution of isolated hearts using a Langendorff apparatus (Li et al. 1996). However, this method is not easily applicable to smaller-sized hearts and impossible for hearts from newborn mice. Therefore, we adapted a method originally used for the isolation of smooth muscle cells (Draeger et al. 1989) to digest cardiac tissue also from newborn mice. Pieces from cardiac muscle tissue are tied at extended length onto plastic strips (see schematic drawing in Fig. 1) and processed for digestion as well as the following washing steps in this state. Afterwards the muscle pieces are cut from the strips and individual cardiomyocytes are released by gentle trituration by pipetting up and down using a wide-mouthed Pasteur pipette. Using this technique we are able to obtain cardiomyocytes that retain their original shape as judged from reconstructions of serial sectioned cryomaterial of hearts taken from newborn mice (Fig. 2). This technique is not only applicable for perinatal stages but also works in later stages including hearts from adult mice. While allowing the isolation of apparently undamaged cardiomyocytes, it is also possible to separate right and left ventricular walls, thereby facilitating separate analysis of growth parameters of right versus left ventricular cardiomyocytes. Using this isolation technique, followed by immunofluorescence staining of the myofibrils as well as the nuclei, we were

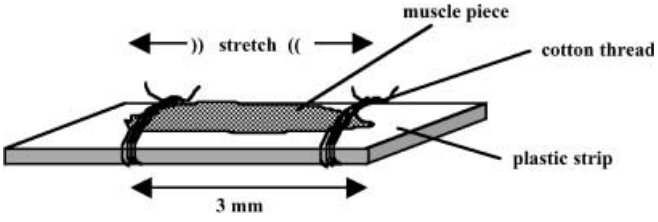

Fig. 1 Schematic drawing of heart muscle pieces (size approximately 1×3 mm) that were tied at extended length with cotton thread onto plastic strips.

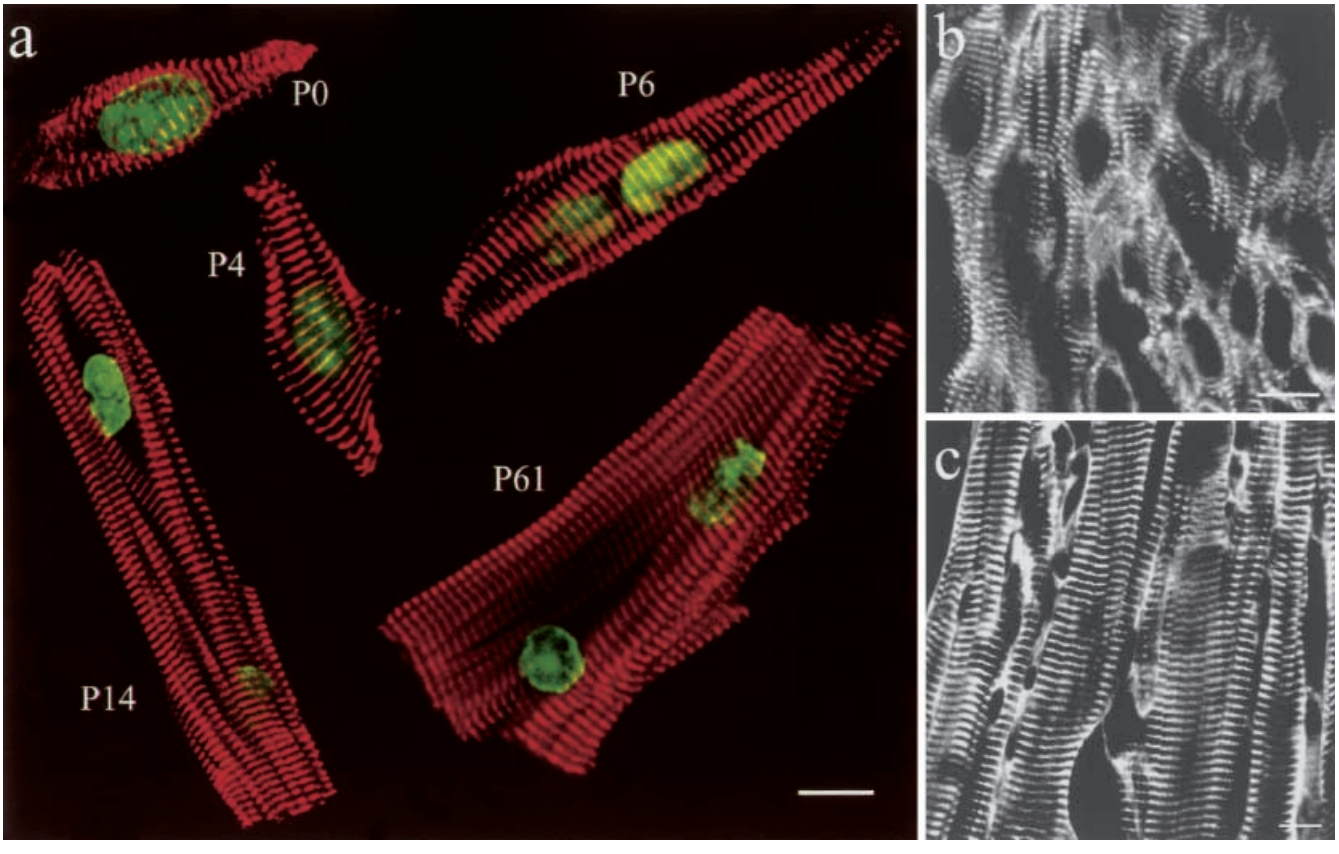

Fig. 2 Fixed freshly isolated mouse cardiomyocytes of different ages (*P0*, *P4*, *P6*, *P14*, *P61*) labelled with an anti-myomesin antibody (in red) and Pico Green (in *green*) as a nuclear stain (**a**). Myomesin is located in the M-band. During the postnatal phase a morphological change from small spindle-shaped cells (P0, P4) to large rod-shaped cells occurs. Additionally from P6 onwards most of the cardiomyocytes contain two nuclei. Cryosections from newborn (**b**) and adult (**c**) heart stained with anti-myomesin antibodies, demonstrating similar shape differences as seen in the freshly isolated cardiomyocytes. *Bar* 10 µm

able to analyse the postnatal growth parameters in the mouse heart by confocal microscopy. Figure 2a shows single confocal sections from freshly isolated cardiomyocytes from P0, P4, P6, P14 and P61 mice. Cardiomyocytes isolated during the first days after birth are characterised by a spindle-like shape and usually have just one nucleus. Between P4 and P6, the cells become more elongated, reach more of a rod-like shape and nuclear division takes place, yielding binucleated cardiomyocytes that are typical for the rodent ventricle. At P14, the rod-like shape is even more pronounced and sarcomeres have been added mainly in the longitudinal direction. By P61 cardiomyocytes have also increased their girth and display their mature morphology, being completely filled with myofibrils and possessing two nuclei. The shape of the freshly isolated cardiomyocytes closely resembles the differences in shape of the cardiomyocytes in tissue at newborn and adult stages, respectively (Fig. 2b, c), excluding potential preparation artifacts.

Determination of cardiomyocyte growth parameters during postnatal development

Data sets from confocal stacks obtained from cardiomyocytes of different developmental stages isolated by the method described above were used to measure the volume as well as analysing growth parameters such as length and width of the cardiomyocytes and the number of sarcomeres using a specialised software, Imaris (Bitplane AG Zurich, Switzerland). A detailed listing of these postnatal growth parameters of the murine heart is given in Table 1. Because our new method allows a separate isolation of cardiomyocytes from the left and the right ventricles, we were able to compare the growth parameters of cardiomyocytes from the two chambers. The general profile of volume increase is quite similar, as depicted in Fig. 3a, with a phase of constant cell volume from birth until P4 and a steep increase in the volume in the 10 following days. Interestingly, although the volume seems to increase in a comparable manner in cardiomyocytes from the left and the right ventricle, a difference in the way how this is achieved was observed. When length to width ratios are compared between LV and RV cardiomyocytes during the first postnatal month it is apparent that while after P5 RV cardiomyocytes increase in length first and grow by lateral addition of myofibrils only after P12, LV show exactly the opposite growth pattern at that time, with first increasing their girth and growing in length only from P12 onwards (Fig. 3b). In the adult animal LV cardiomyocytes are longer compared to RV cardiomyocytes, which in their turn show increased widths, resulting in similar volumes for both types of cardiomyocytes. At the moment it is completely unclear how this different growth behaviour is regulated but it is likely that it reflects the different demands on the right and left ventricular chambers during development.

A comparison between the developmental profile of the cardiomyocyte volume increase with the heart weight

Table 1 Morphometric characteristics of freshly isolated myocytes from mouse hearts (values are means ± SD; *CV LV* cell volume of left ventricle; *CV RV* cell volume of right ventricle; *BW* body weight; *HW* heart wet weight; *TL* tibia length; *CL LV* cell length of left ventricle; *CL RV* cell length of right ventricle; *CW LV* cell width of left ventricle; *CW RV* cell width of right ventricle; *CT LV* cell thickness of left ventricle; *CT RV* cell thickness of right ventricle; *S LV* number of sarcomeres in left ventricle; *S RV* number of sarcomeres in right ventricle; *n.d.* not determined; * average of two independent data sets; † average of at least five measurements; ‡ only two data points; § average of only one data set; ‖ only one data point)

Parameter	Age (in days)										
	0	4	5	6	7	11	14	22	31	61	205
CV LV* (µm³)	1570±584	1820±441	2217±661	2980±570	3338±670	5186±807	7479±1187	8362±1622	10070±1861	18306±3439§	24306±4675§
CV RV* (µm³)	1754±606	1862±492	2022±516	2924±509	3375±955	5174±1309	6973±1844	7952±1923	9314±1779	17370±2790§	25859±3811§
BW† (g)	1.5±0.1	2.4±0.3	3.6±0.3	4.6±0.3	5.2±0.4	7.9±0.7	8.2±0.9	12.9±1.2‡	16.1±1.1‡	24.3‖	28.5‖
HW† (mg)	8.0±1.0	12.7±1.7	18.2±3.0	22.7±2.7	24.7±4.1	35.6±2.3	51.8±9.2	n.d.	n.d.	n.d.	n.d.
TL† (mm)	2.7±0.3	3.9±0.6	4.8±0.2	5.8±0.3	6.4±0.2	8.2±0.5	9.3±0.5	n.d.	n.d.	n.d.	n.d.
CL LV* (µm)	46.1±13.3	49.3±10.1	45.6±11.6	52.2±7.7	50.9±8.1	60.1±10.0	71.3±12.4	70.1±11.9	72.5±10.9	66.3±8.9§	128.0±33.6§
CL RV* (µm)	45.2±7.2	41.4±8.2	45.0±7.5	50.8±5.7	54.6±12.2	55.9±12.6	61.9±13.2	65.1±9.4	68.9±9.1	86.6±10.9§	85.2±11.7§
CW LV* (µm)	13.5±2.4	14.0±2.9	13.6±2.6	15.5±3.2	16.3±2.4	17.9±3.6	17.8±2.1	17.9±3.5	25.2±5.5	29.4±7.5§	28.7±7.8§
CW RV* (µm)	15.0±3.7	14.5±2.5	13.9±2.8	15.8±2.2	15.7±3.3	16.0±2.0	19.3±4.5	19.1±3.5	20.7±5.3	28.4±5.1§	35.8±4.2§
CT LV* (µm)	4.7±0.8	5.3±1.2	6.8±1.3	6.8±1.2	7.1±1.1	8.7±1.6	10.7±1.5	10.9±1.8	8.9±1.9	14.4±2.2§	10.6±3.0§
CT RV* (µm)	4.9±0.7	6.0±1.0	6.1±1.0	6.6±1.2	6.8±1.4	10.1±1.4	10.5±1.7	10.9±1.2	9.9±1.5	12.1±2.9§	11.6±2.6§
S LV*	32±6	34±5	42±7	47±4	49±6	55±6	61±7	60±5	63±7	56±4§	80±15§
S RV*	34±4	35±5	42±5	49±5	50±8	52±7	57±9	58±7	59±8	67±6§	63±10§

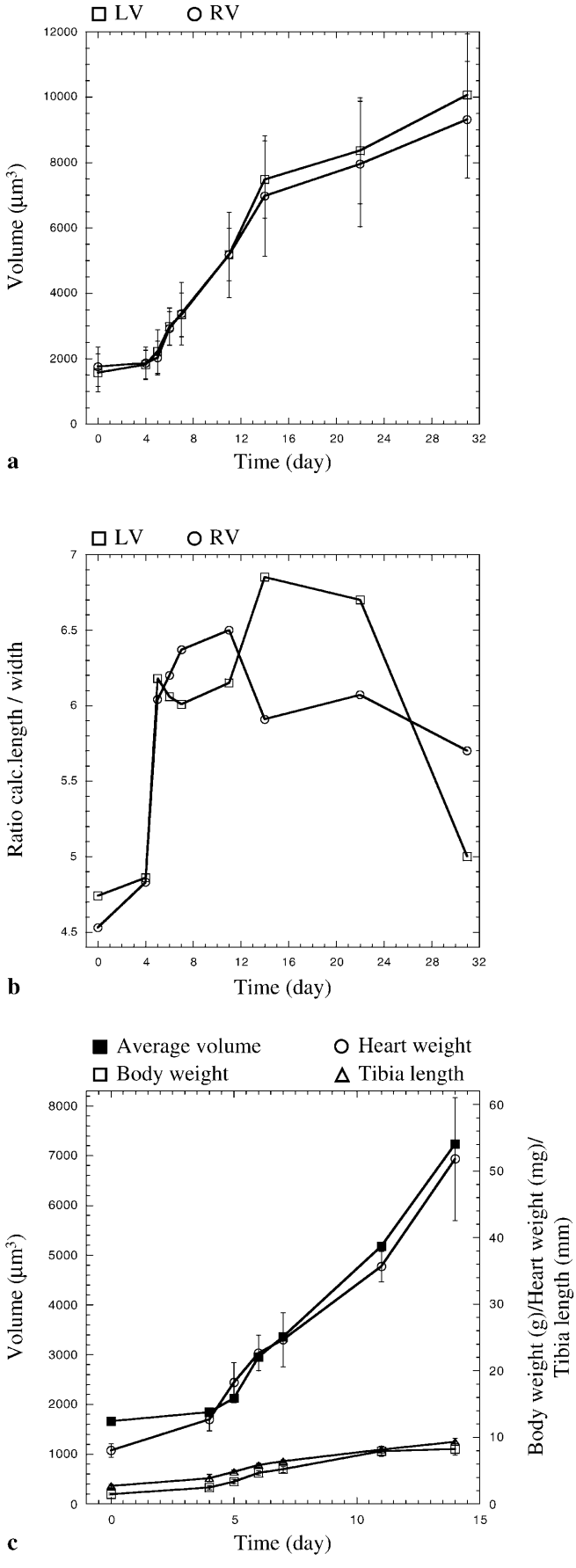

is depicted in Fig. 3c. Within the first 4 postnatal days the heart weight increases while the volume of the cardiomyocytes remains constant, indicating that growth still occurs mainly due to hyperplasia during the first postnatal days also in the mouse. At P4 the period of hypertrophic growth sets in with a steep rise in cardiomyocyte volume that lasts until about P14, when the increment declines to reach a plateau at about P61. The curves for the volume and the heart weight overlap exactly after P4, suggesting that from then onwards gain in heart mass is only due to increase in cardiomyocyte volume, the phase of so-called developmental hypertrophy.

When the increase in heart weight is compared with the body weight at the same time it is apparent that in order to meet the increasing demands, the heart has to grow much more in relation to the body weight. To show that this is not due to differences in food intake, tibia length was analysed as a more reliable marker at the same time, resulting in a curve that is almost overlapping with the body weight (Fig. 3c).

These results show that this novel isolation method and the subsequent analysis in the confocal microscope after immunostaining could provide the parameters of postnatal cardiomyocyte growth in the mouse. The main phase of volume increase starts after P4, similar to data observed in the rat (Li et al. 1996). Although the overall volume increase is similar between cardiomyocytes from the left and the right ventricles, there are differences in the first 2 postnatal weeks in the way how this is achieved by either lateral or longitudinal addition of sarcomeres.

Growth characteristics of cardiomyocytes from MLP knockout mice

Numerous mouse models for cardiomyopathies have been created in recent years either by genetic methods or by induction of stenosis by operation techniques (Geisterfer-Lowrance et al. 1996; Arber et al. 1997; Patten et al. 1998; Sussman et al. 1998; Yang et al. 1998; Muthuchamy et al. 1999; Ding et al. 2000), reviewed, e.g. in (Izumo and Shioi 1998; Dalloz et al. 2001). With the

Fig. 3 Volume of freshly isolated cardiomyocytes from mouse heart (**a**). Around postnatal day 4, myocyte volume progressively increases and after 2–3 weeks the rate of increase is again reduced. Each *point* is the mean of at least 14 cardiomyocytes. The *curves* represent the average of two independent data set measurements for left and right ventricles. Relative ratio of length to width growth of freshly isolated mouse cardiomyocytes (**b**). The changing slope of the line indicates alternating growth in length and width during different phases. Length is the calculated product of numbers of sarcomeres using an average sarcomere length in heart of 2 µm. See Table 1 for mean values ± SD. *LV* left ventricle (*square*), *RV* right ventricle (*circle*). Comparison of volume of freshly isolated cardiomyocytes (*filled square*), body weight (*open square*), heart weight (*circle*) and tibia length (*triangle*) during development (**c**). Body weight and tibia length are continuously increasing. The volume and the heart weight curve behave similar except between P0 and P4. The difference in the early postnatal days may be due to still-ongoing cell division

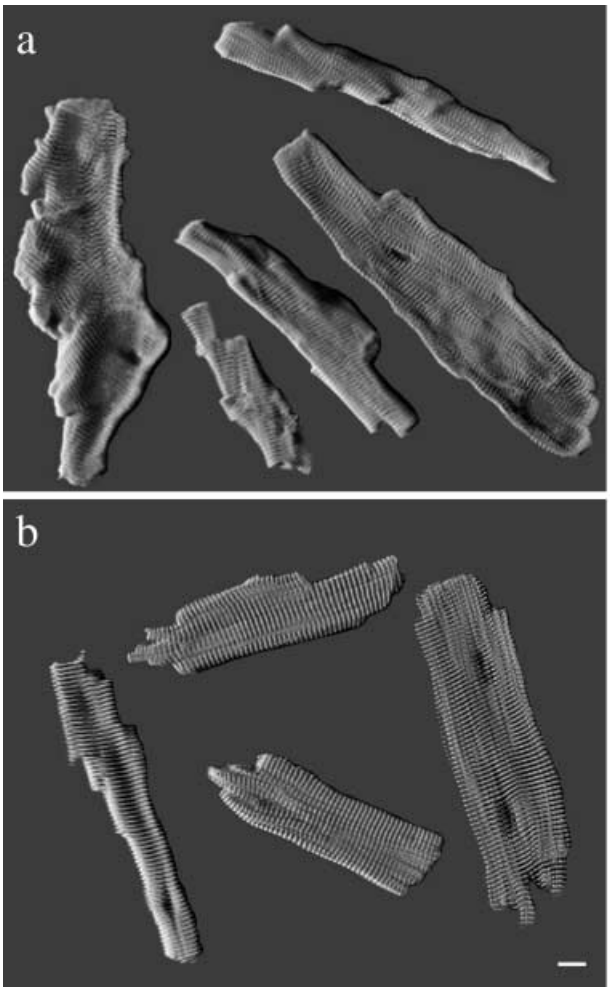

c

Parameter	Age (in days)			
	0	7	14	205
MLP				
CV* (μm^3)	1222 ± 610	3876 ± 1061	7853 ± 1425	28420 ± 14866
Min (μm^3)	576	2478	5659	12523
Max (μm^3)	2868	6904	11654	68452
wt				
CV* (μm^3)	1662 ± 593	3359 ± 833	7234 ± 1532	25083 ± 4147
Min (μm^3)	808	2006	4606	19338
Max (μm^3)	3121	5477	10779	33064

Values are means±SD; CV, cell volume; Min, smallest volume; Max, largest volume; MLP, muscle LIM protein; wt, wild-type; * average of left and right ventricle.

Fig. 4 Fixed freshly isolated adult mouse cardiomyocytes from (**a**) MLP knock-out mice and (**b**) wt mice stained with an anti-myomesin antibody. Myomesin is located in the M-band. Individual MLP cardiomyocytes show a high degree of heterogeneity in their morphology and size compared to the wt cells. Cell volume of freshly isolated cardiomyocytes from MLP knock-out mice compared with wt mice (**c**). *Bar* 10 µm

availability of the data for wildtype mice as discussed here, it is now possible to compare eventual altered growth characteristics in these diseased mice. In a first attempt we analysed the growth characteristics of cardiomyocytes obtained from MLP knockout mice, a mouse model for dilated cardiomyopathy. Freshly isolated cardiomyocytes from adult MLP knockout mice are characterised by their more irregular shape with myofibrils not running strictly in parallel as in the wildtype (Fig. 4b) but at slightly oblique angles to each other (Arber et al. 1997; Fig. 4a). The representative selection of cardiomyocytes from MLP knockout versus wildtype mice indicated also another typical feature, namely a high variability in size in cardiomyocytes isolated from MLP knockout mice whereas wildtype cardiomyocytes show only little variation in their volume. These morphological observations are substantiated by volume analysis of confocal data stacks, where cardiomyocytes obtained from adult wild-type mice have an average volume of 25083 µm^3 with a SD of ± 4147 (16.5%), while cardiomyocytes from MLP knockout mice display volumes ranging from 12523 µm^3 to 68452 µm^3, yielding an average size of 28420 µm^3 but a SD of ± 14866 (52.3%). By staining for an intracellular intercalated disk protein, beta-catenin, it was verified that the measured cardiomyocytes were indeed individual cardiomyocytes and not a pair of partially digested cardiomyocytes (data not shown). This high variability in volume becomes only apparent in the adult MLP knockout mice. When volumes from newborn cardiomyocytes are compared, cardiomyocytes from MLP knockout mice are smaller than those from WT, with an average value of 1222 µm^3 versus 1662 µm^3 for the wildtype; however, the values at P7 and P14 are rather similar, with the cardiomyocytes from the MLP knockout mice being slightly larger than wildtype cardiomyocytes, but showing a comparable SD. Therefore the high variability in size is only a characteristic feature of cardiomyocytes from adult MLP knockout mice. This is similar to the alterations observed at the intercalated disk in the MLP knockout mouse which also become only apparent in adult animals (Ehler et. al. 2001). The high variation in cardiomyocyte volume in the adult suggests that the hypertrophic response is deregulated in this kind of cardiomyopathic mice at later developmental stages. Together with the fibrosis that was observed and the more irregular shape resulting in a higher number of cell – cell contacts, the large differences in cardiomyocyte size might well result in the heart insufficiency and reduced output that is observed in MLP knockout mice.

Discussion

The results presented here are the first detailed analysis of postnatal cellular growth parameters in the murine

heart. With our novel isolation method we were not only able to isolate cardiomyocytes from newborn mice that have an overall shape that is comparable to that in situ as judged by the analysis of serial frozen sections, but also to obtain separate data sets for cardiomyocytes from the left and the right ventricles. Comparison of the obtained growth curves with data obtained from postnatal rat heart shows that the growth parameters are very similar (Li et al. 1996). Also in the rat an abrupt change from hyperplastic to hypertrophic growth takes place at around postnatal day 3 (Li et al. 1996). After that a dramatic increase in volume was observed, accompanied by binucleation in the first postnatal week (Li et al. 1996). Analysis of postnatal division of cardiac cells in mice by Bromo-deoxyuridine (BrdU) labelling revealed a drastic decrease in incorporation after the first postnatal week as well (Machida et al. 1997). In agreement with Li et al. for the rat we found no evidence for cell division also in the adult mouse heart (Li et al. 1996). In 20-day-old mice less than 1% BrdU-positive cells could be identified in the heart; however their identity as true cardiomyocytes remains to be shown (Machida et al. 1997). This complete cessation of cardiomyocyte proliferation activity is in contrast to chicken, where division could also be observed in adult cardiomyocytes (Li et al. 1997).

So far no detailed analysis of postnatal mouse cardiomyocyte volumes has been published. However, when we compare the sizes we determined with our isolation method with values that were published for single developmental stages, they are within a similar range. For example, from desmin knockout mice, which show features of dilated cardiomyopathy (Milner et al. 2000), cardiomyocytes were isolated that had an average length of 142.6 µm compared with wildtype of 139.7 µm with a diameter of 29.7 and 29.9 µm, respectively, which compares well with the length of 128.0 (LV) and 85.2 (RV) µm and the width of 28.7 (LV) and 35.8 (RV) µm that we observe in our measurements. Similarly, measurements from a mouse strain that is transgenic for a truncated cardiac troponin T and serves as a model for familial hypertrophic cardiomyopathy (Tardiff et al. 1998), gave values of a length of 134.5 µm for the non transgenic compared to 114.3 µm for the transgenic strain with a width of 30.6 and 26.7 µm, respectively. A possible cause for the shorter length of our cardiomyocytes is their partial contraction during the paraformaldehyde fixation; however, since this would then lead to an increased thickness it has no effect on the volume measurements. The results obtained in mice are remarkably similar to different measurements performed on cardiomyocytes from humans suffering from several diseases (reviewed in Poole-Wilson 1995), where lengths were observed that range from 36 µm to 197 µm with an average length ranging around 110 µm. The high variability is probably due to different isolation techniques, different fixation protocols as well as different methods of volume determination. Based on our observations that the values that we calculate roughly for the cardiomyocytes from reconstituted frozen sections of heart are rather similar in the adult as well as in the newborn animals (data not shown) we do not think that our isolation technique selects just for a subset of cardiomyocytes. Also the fact that the values that we obtain in our measurements are comparable with the values published previously and obtained by other isolation techniques such as Langendorff perfusion suggest that we get an overview over the whole spectrum of ventricular cardiomyocytes.

In addition to the possibility of isolating undamaged cells in their original shape even from newborn mouse hearts, our technique offers several additional advantages. First, it allows the separation of left and right ventricular wall, and would even allow a separate analysis of septal cardiomyocytes, which we did not perform in this contribution. Secondly, using this technique cardiomyocytes can also be isolated from rather small tissue samples and after some adaptation even an isolation from material obtained by biopsies could be envisaged. This is especially important since previous studies have indicated that the overall shape of cardiomyocytes is altered in the diseased heart (Arber et al. 1997; Ehler et al. 2001). Thirdly, in contrast to an isolation method proposed by Gerdes' group, where rod-shaped cardiomyocytes are isolated by KOH digestion from formalin-fixed material (Tamura et al. 1998) immunostaining is possible, so that a qualitative analysis of the protein expression profile of the isolated cardiomyocytes can be performed, including the staining for intercalated disk proteins to ensure true separation of individual cardiomyocytes or the staining for marker proteins for, e.g. hypertrophy.

Investigating a mouse model for dilated cardiomyopathy, the MLP knockout mice with this isolation method, we observed that MLP knockout cardiomyocytes have a much more irregular growth pattern than the heart cells of wildtype mice, which is also reflected in the not well aligned myofibrils. The results on the heterogeneity of volumes in the adult MLP knockout mice suggest that during the development of the phenotype of dilated cardiomyopathy a deregulation of control of cellular growth happens in these mice. So far the exact pathways that control a hypertrophic response are unclear and a scenario of a complex combinatorial action of several signalling pathways is the most likely (Hefti et al. 1997). It will be important to find out which of these pathways is not fully functional in the MLP knockout mouse, thus resulting in this high variation of volumes that is observed. This variation in cellular size is probably one of the reasons for myocyte disarray and the increased number of contacts that are observed (Ehler et. al. 2001). It has been suggested previously that the ventricular wall thinning that is observed in dilated cardiomyopathy might be either caused by myocyte lengthening (Gerdes and Capasso 1995) or by side to side slippage of cells within the wall (Beltrami et al. 1995). Our results together with the observations made by others (Schaper et al. 1995) indicate that possibly also a wide range of cardiomyocyte size and the resulting misalignment can contribute to the changes in wall thickness. The fact that differences in

cardiomyocyte size are only apparent in the adult and not during the first 2 postnatal weeks of development is reminiscent of the alterations that have been observed in intercalated disk composition in the MLP knockout mice, which also only become prominent in the adult stage (Ehler et. al. 2001).

In summary, the data reported here provide an important basis for the analysis and comparison of growth parameters in different mouse models for cardiomyopathy. Additionally the sharp transition of hyperplastic to hypertrophic growth that is also seen in the mouse heart would allow the identification of factors that distinguish these two stages by comparison of the two mRNA/protein pools by subtractive hybridisation or analysis of 2D-gel protein patterns, respectively.

Acknowledgements This work was supported by a predoctoral training grant from the ETH (20-356-97), a grant from the Swiss National Science Foundation to JCP (31.52417/97) and a fellowship from the Fondation G.+S. Prévot, Geneva, Switzerland. Special thanks goes to Stephan Lange for help with the artwork.

References

Arber S, Hunter JJ, Ross JJ, Hongo M, Sansig G, Borg J, Perriard JC, Chien KR, Caroni P (1997) MLP-deficient mice exhibit a disruption of cardiac cytoarchitectural organization, dilated cardiomyopathy, and heart failure. Cell 88:393–403

Beinlich CJ, Rissinger CJ, Morgan HE (1995) Mechanisms of rapid growth in the neonatal pig heart. J Mol Cell Cardiol 27: 273–281

Beltrami CA, Finato N, Rocco M, Feruglio GA, Puricelli C, Cigola E, Sonnenblick EH, Olivetti G, Anversa P (1995) The cellular basis of dilated cardiomyopathy in humans. J Mol Cell Cardiol 27:291–305

Campbell SE, Gerdes AM, Smith TD (1987) Comparison of regional differences in cardiac myocyte dimensions in rats, hamsters, and guinea pigs. Anat Rec 219:53–59

Clubb FJ Jr, Bishop SP (1984) Formation of binucleated myocardial cells in the neonatal rat. An index for growth hypertrophy. Lab Invest 50:571–577

Dalloz F, Osinska H, Robbins J (2001) Manipulating the contractile apparatus: genetically defined animal models of cardiovascular disease. J Mol Cell Cardiol 33:9–25

Ding B, Price RL, Goldsmith EC, Borg TK, Yan X, Douglas PS, Weinberg EO, Bartunek J, Thielen T, Didenko VV, Lorell BH (2000) Left ventricular hypertrophy in ascending aortic stenosis mice: anoikis and the progression to early failure. Circulation 101:2854–2862

Draeger A, Stelzer EH, Herzog M, Small JV (1989) Unique geometry of actin-membrane anchorage sites in avian gizzard smooth muscle cells. J Cell Sci 94:703–711

Ehler E, Horowits R, Zuppinger C, Price RL, Perriard E, Leu M, Caroni P, Sussman M, Eppenberger HM, Perriard JC (2001) Alterations at the intercalated disk associated with the absence of muscle LIM protein. J Cell Biol 153:763–772

Geisterfer-Lowrance AA, Christe M, Conner DA, Ingwall JS, Schoen FJ, Seidman CE, Seidman JG (1996) A mouse model of familial hypertrophic cardiomyopathy. Science 272:731–734

Gerdes AM, Capasso JM (1995) Structural remodeling and mechanical dysfunction of cardiac myocytes in heart failure. J Mol Cell Cardiol 27:849–856

Grove BK, Kurer V, Lehner C, Doetschman TC, Perriard JC, Eppenberger HM (1984) Monoclonal antibodies detect new 185,000 Dalton muscle M-Line protein. J Cell Biol. 98:518–524

Hefti MA, Harder BA, Eppenberger HM, Schaub MC (1997) Signaling pathways in cardiac myocyte hypertrophy. J Mol Cell Cardiol 29:2873–2892

Izumo S, Shioi T (1998) Cardiac transgenic and gene-targeted mice as models of cardiac hypertrophy and failure: a problem of (new) riches. J Card Fail 4:263–270

Legato MJ (1979) Cellular mechanisms of normal growth in the mammalian heart. I. Qualitative and quantitative features of ventricular architecture in the dog from birth to five months of age. Circ Res 44:250–262

Li F, Wang X, Capasso JM, Gerdes AM (1996) Rapid transition of cardiac myocytes from hyperplasia to hypertrophy during postnatal development. J Mol Cell Cardiol 28:1737–1746

Li F, McNelis MR, Lustig K, Gerdes AM (1997) Hyperplasia and hypertrophy of chicken cardiac myocytes during posthatching development. Am J Physiol 273:R518–526

Machida N, Brissie N, Sreenan C, Bishop SP (1997) Inhibition of cardiac myocyte division in c-myc transgenic mice. J Mol Cell Cardiol 29:1895–1902

Messerli M, Eppenberger ME, Rutishauser B, Schwarb P, Arx P von, Koch-Schneidemann S, Eppenberger HM, Perriard J-C (1993a) Remodeling of cardiomyocyte cytocarchitecture visualized by 3D confocal microscopy. Histochemistry 100:193–202

Messerli JM, Voort HT van der, Rungger Brandle E, Perriard JC (1993b) Three-dimensional visualization of multi-channel volume data: the amSFP algorithm. Cytometry 14:725–735

Milner DJ, Mavroidis M, Weisleder N, Capetanaki Y (2000) Desmin cytoskeleton linked to muscle mitochondrial distribution and respiratory function. J Cell Biol 150: 1283–1298

Muthuchamy M, Pieples K, Rethinasamy P, Hoit B, Grupp IL, Boivin GP, Wolska B, Evans C, Solaro RJ, Wieczorek DF (1999) Mouse model of a familial hypertrophic cardiomyopathy mutation in alpha- tropomyosin manifests cardiac dysfunction. Circ Res 85:47–56

Oberpriller JO, Oberpriller JC (1974) Response of the adult newt ventricle to injury. J Exp Zool 187:249–253

Patten RD, Aronovitz MJ, Deras-Mejia L, Pandian NG, Hanak GG, Smith JJ, Mendelsohn ME, Konstam MA (1998) Ventricular remodeling in a mouse model of myocardial infarction. Am J Physiol 274:H1812–1820

Poole-Wilson PA (1995) The dimensions of human cardiac myocytes; confusion caused by methodology and pathology. J Mol Cell Cardiol 27 863–865

Rothen-Rutishauser BM, Ehler E, Perriard E, Messerli JM, Perriard J-C (1998) Different behaviour of the non-sarcomeric cytoskeleton in neonatal and adult rat cardiomyocytes. J Mol Cell Cardiol 30:19–31

Rumyantsev PP (1977) Interrelations of the proliferation and differentiation processes during cardiact myogenesis and regeneration. Int Rev Cytol 51:186–273

Schaper J, Hein S, Scholz D, Mollnau H (1995) Multifacetted morphological alterations are present in the failing human heart. J Mol Cell Cardiol 27:857–861

Smolich JJ, Walker AM, Campbell GR, Adamson TM (1989) Left and right ventricular myocardial morphometry in fetal, neonatal, and adult sheep. Am J Physiol 257:H1–9

Sussman MA, Welch S, Cambon N, Klevitsky R, Hewett TE, Price R, Witt SA, Kimball TR (1998) Myofibril degeneration caused by tropomodulin overexpression leads to dilated cardiomyopathy in juvenile mice. J Clin Invest 101:51–61

Tamura T, Onodera T, Said S, Gerdes AM (1998) Correlation of myocyte lengthening to chamber dilation in the spontaneously hypertensive heart failure (SHHF) rat. J Mol Cell Cardiol 30: 2175–2181

Tardiff JC, Factor SM, Tompkins BD, Hewett TE, Palmer BM, Moore RL, Schwartz S, Robbins J, Leinwand LA (1998) A truncated cardiac troponin T molecule in transgenic mice suggests multiple cellular mechanisms for familial hypertrophic cardiomyopathy. J Clin Invest 101: 2800–2811

Yang Q, Sanbe A, Osinska H, Hewett TE, Klevitsky R, Robbins J (1998) A mouse model of myosin binding protein C human familial hypertrophic cardiomyopathy. J Clin Invest 102:1292–1300